SIMULATION OF A SOLAR FUNNEL COOKER USING MATLAB

Rafael Cubero-Leiva[1,3], Fernando Domínguez-Muñoz[1],

Celestino R. Ruivo[2] and Francisco R. Villatoro[3] *

1: Departamento de Ingeniería Mecánica, Térmica y de Fluidos, Escuela de Ingenierías Industriales,
Universidad de Málaga, Ampliación del Campus de Teatinos, s/n, 29071, Málaga, Spain
e-mail: fdominguezm@uma.es, web: http://webdeptos.uma.es/mmt/

2: Departamento de Engenharia Mecânica, Universidade do Algarve, Faro, Portugal
e-mail: cruivo@ualg.pt web: http://solarcooking.wikia.com/wiki/Celestino_Ruivo

3: Departamento de Lenguajes y Ciencias de la Computación, Escuela de Ingenierías Industriales,
Universidad de Málaga, Ampliación del Campus de Teatinos, s/n, 29071, Málaga, Spain
e-mail: frvillatoro@uma.es web: http://www.lcc.uma.es/

Abstract: *A software for the calculation of the radiation heat transfer in solar funnel cookers by means of the radiosity method has been developed in Matlab. The software has been used to study a folding solar cooker. The cooker geometry is discretized using a triangular mesh where a piecewise constant approximation is assumed for the radiosity function. Form factors, including self-occlusions, are calculated by properly refining the triangular mesh. The concentration factor of the solar cooker is estimated as a function of its position and orientation with respect to that of the Sun.*

Keywords: Solar Cooker, Concentration factor, Numerical model, Radiation heat transfer, Radiosity method.

1. INTRODUCTION

A solar panel cooker uses a multifaceted mirror to concentrate sunlight from above in a cooking vessel placed at its focus inside a clear, transparent enclosure, to create a greenhouse effect [1,2,3]. Funnel cookers are simple to construct, store and transport, so they result in low-cost, effective cooking kits. The simulation of the thermal heat transfer in a flat plate collector will help the development of optimal designs and recommendation practices for the best performance. Most mathematical models for the numerical simulation of solar cookers use heat balance equations for the each component of the cooker [4]. They are not able to determine the distribution of the concentrating irradiance on the surface of the cooking vessel.

The radiative heat transfer in a funnel cooker can be calculated by means of using ray-tracing and radiosity methods [5,6]. Both methods determine the direct irradiation from the Sun and the indirect irradiation from the sky, including the effect of self-shadowing and the exchange of radiative energy between the surfaces of the cooker. The selection between ray-tracing and radiosity for the simulation of solar cookers is a matter of personal preference. The main disadvantage of the ray-tracing method is that Monte Carlo techniques are required for indirect irradiation, resulting in an increase of the computational cost. On the other side, the main disadvantage of radiosity is that the sky and the Sun are projected into a finite volume enclosure. In practice, both methods are expected to yield similar irradiance maps on the panels of the solar cooker and the surface of the cooking vessel, which can be compared with those obtained by reciprocal optical tests [7] and by other simulation methods, as those used for box solar cookers [8].

On the best of the authors' knowledge, the radiosity method has not been used in the simulation of the solar cookers, in fact, the ray-tracing has been used only for box solar cookers [9]. In this paper, preliminary results for the simulation of panel solar cookers using the radiosity method are presented; the concentration factor for the cooking vessel is calculated comparing the results with and without the solar cooker as a function of the position of the Sun in the sky. Section 2 recalls the radiosity method and the form factor calculation. Section 3 describes the geometry of the solar funnel cooker used to obtain in the results presented in Section 4. Finally, Section 5 summarizes our main conclusions.

2. RADIOSITY METHOD

The radiosity equation describes the amount of energy emitted by a surface as the sum of the inherent emission of the surface (for heat sources) and the reflected energy on the surface (dependent of its reflectivity coefficient) from all the energy that it receives from all other surfaces [5,6]. A map of the thermal radiation over all the surfaces can be determined by solving the radiosity equation by means of the finite element method.

The standard implementation of the radiosity method starts with a discretization of the surface of all the objects into triangular elements over which a piecewise constant approximation is used for the radiosity function. Therefore, the integral equation is rewritten into a linear system of equations for the unknown constant values of the radiosity in every element. The radiosity equation can be written as

$$B_i = E_i + \rho_i \sum_{j=1}^{n} F_{ij} B_j, \qquad (1)$$

where B_i is the radiosity at the i-th surface, E_i is its emissivity, ρ_i is its reflectivity, and F_{ij} is the form factor between the i-th and j-th surfaces, i.e., the ratio of energy received by the i-th surface from the total energy emitted by the j-th surface. The matrix representation of Eq. (1) is given by

$$
\begin{matrix}
1 - \rho_1 F_{11} & -\rho_1 F_{12} & \cdots & -\rho_1 F_{1n} \\
-\rho_2 F_{21} & 1 - \rho_2 F_{22} & & -\rho_2 F_{2n} \\
\vdots & \vdots & \ddots & \vdots \\
-\rho_n F_{n1} & -\rho_n F_{n2} & \cdots & 1 - \rho_n F_{nn}
\end{matrix}
\begin{matrix}
B_1 \\ B_2 \\ \vdots \\ B_n
\end{matrix}
=
\begin{matrix}
E_1 \\ E_2 \\ \vdots \\ E_n
\end{matrix} ,
$$

which can be easily solved by using Matlab's set of iterative methods. The irradiance radiosity (the energy incoming into every geometrical element) is given by

$$ G_i = \sum_{j=1}^{n} F_{ij} B_j . \tag{2} $$

The exact calculation of the form factors F_{ij} requires the numerical calculation of the following equation

$$ F_{ij} = \frac{1}{A_i} \int_{A_i} \int_{A_j} \frac{\cos \theta_i \cos \theta_j}{\pi r^2} V_{ij} \, dA_i \, dA_j , \tag{3} $$

where A_i is the area of the i-th surface, θ_i is the angle with respect to the normal vector of the i-th surface of the vector connecting the centers of surfaces A_i and A_j, and V_{ij} is the visibility function (the amount of area A_i visible from the center of the area A_j). Equation (4) is numerically evaluated by means of a simple quadrature method; concretely, every area is divided in small elements where the visibility function is either 1 or 0, and the differential form factor is approximated by

$$ dF_{A_i \to A_j} = \frac{\cos \theta_i \cos \theta_j}{\pi r^2} V_{ij} A_j , $$

where the sum of these differential form factors yields the form factor F_{ij}.

For solar cookers the most important design factor is the concentration ratio, given by

$$ CR = \frac{G_{total} \, (with \, cooker)}{G_{total} \, (without \, cooker)} , \tag{4} $$

i.e., the quotient of the total irradiance of the cooking vessel calculated with and without the concentrator cooker; the total irradiance is obtained by using

$$ G_{total} = \frac{\sum_i A_i G_i}{\sum_i A_i} , $$

where Eq. (3) applied to the solution of Eq. (1).

3

3. SOLAR FUNNEL COOKER

This paper presents preliminary results obtained by using a prototype software for the simulation of arbitrary solar cookers by means of using the radiosity method. This prototype has been developed by the first author as part of his M.E. thesis. This software is currently under further development, so here we only present an initial exploration of its potential for the thermal analysis of solar cookers.

Figure 1. Pictures of a solar funnel cooker by Teong Tan [10] (top), of a transparent enclosure (bottom left) and a black cooking vessel (bottom right).

Figure 1 shows pictures of a panel solar cooker (top), a cooking vessel (bottom right) and a transparent enclosure to use the greenhouse effect (bottom left). Our software input is a text file with the description of the polygonal geometry of these three objets. Instead of simulating an existent solar funnel, like the one shown in Fig. 1 (top), from Teong Tan [10], or that used by Celestino Ruivo [11], we have preferred a simplified design. Future work will use their designs in order to compare the predictions of our software with experimental measurements using thermographic cameras.

Figure 2 (left) shows the polygonal geometry of the solar funnel cooker used in the simulations reported in next section of this paper. We also have simplified the cooking vessel up to the extreme; Fig. 2 (center) shows the polygonal shapes of the transparent enclosure and Fig. 2 (right) that of the cooking vessel. Obviously, our results are expected to be highly dependent on this simplification; current work in progress will use rounded versions of these vessels by taking into account a large number of polygons (in our current prototype it is very easy to specify a detailed geometry using the input text files, however we have not developed yet a graphical interface for the automatic introduction of the geometry).
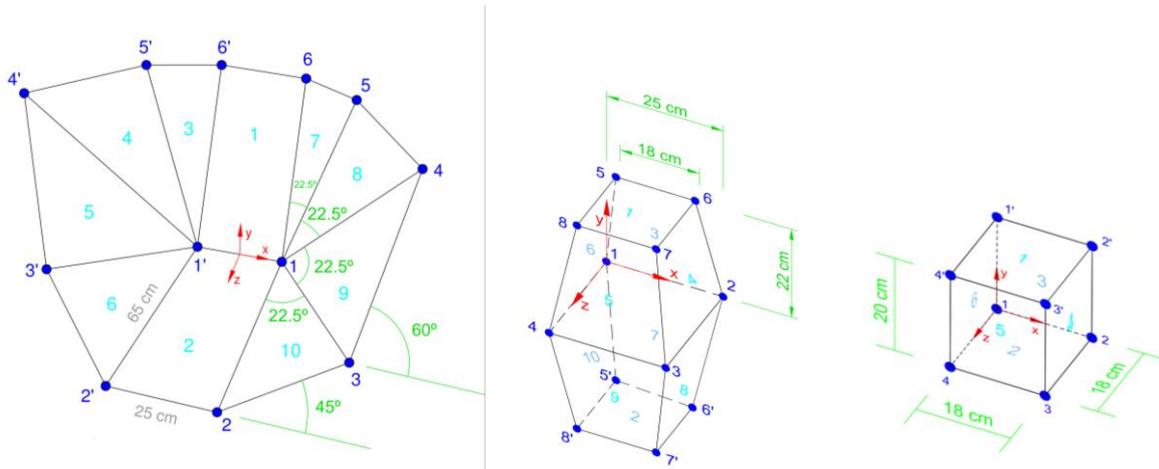
Figure 2. Geometry of the solar funnel cooker simulated in this paper (left),
the transparent enclosure (centre) and the cooking vessel (right).

The radiosity method requires that the solar cooking is inside a global enclosure. In our software the hemispherical sky and the circular solar spot are approximated by using a prism and a square solar spot, respectively, as shown in Fig. 3. The area of the projection of the Sun is adjusted as a function of the size of the global enclosure. In our simulation the sky and the Sun are reflectionless emitters. The total solar irradiance in a sunny day of about $E_T = 1000 \text{ W/m}^2$ can be distributed between the Sun (E_S) and the sky (E_K) such that $E_S + E_K = E_T$. Obviously in sunny days it is expected that $E_S = E_T$., but in a cloudy day there is a non-null contribution of the sky ($E_K \neq 0$).
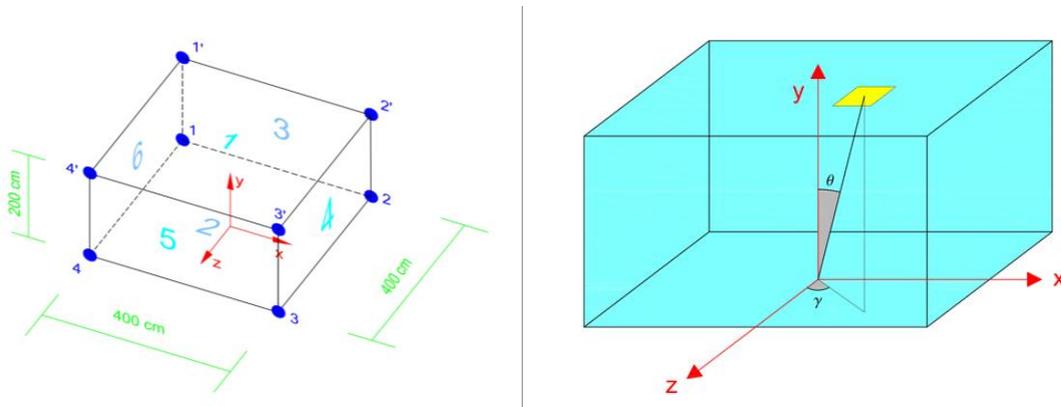
Figure 3. Geometry of the global enclosure of the scene (left) and Sun angular location (right).

4. PRESENTATION OF RESULTS

In the current state of development of our software, only a prototype yet to be validated by comparison with experimental data, our results must be considered as preliminary. Here on we only summarize the extensive set of simulations done by first author in his M.E. Thesis. Our software allows the variation of a large number of parameters of the solar cooking scenery. The panel solar cooker can be rotated

with respect to its own axis (centered on the base polygon) and the inclination of the angle of the cooker back panel can be changed in order to focus more or less radiation on the cooking vessel. The position of the cooking vessel inside the transparent enclosure vessel and its height with respect to the base of the cooker can also be changed. The position of the Sun in the sky and the percentage of radiation associated to the faces of the sky enclosure can be controlled in a one by one basis. Finally, the number of triangle elements in which every polygon is divided for the radiosity calculation and that for the form factor estimation can also be specified independently for every object in the scene.

Figure 4 (left) shows a representative result for the concentration ratio calculated using Eq. (4) on the transparent enclosure vessel, cf. Fig. 2 (center), as a function of the position of the Sun in the sky, determined by the angles θ and γ as shown in Fig. 3 (right), when the Sun is the only source of irradiation (there is no emission from the sky). The back panel of the cooker has an inclination of 100° and every polygon is divided in 16 triangular elements for the calculation of the radiosity. The black (asterisk marked) curve in Fig. 4 (left) corresponds to the summer season, when the Sun is high in the sky; the largest concentration factor is obtained when the solar cooker faces the Sun, with $\theta = 15°$; this angle changes as the inclination of the back angle of the cooker does. The red (circle marked) curve in Fig. 4 (left) corresponds to autumn and spring seasons, when the Sun is a little lower in the sky; the concentration factor depends on the hour of the day, decreasing as the Sun approaches either sunrise or sunset. Finally, the blue (plus sign marked) curve in Fig. 6 (left) illustrates a winter season situation; the self-shadowing of the cooker, and the shadows of the cooker into the cooking vessel result in poor performance; moreover, when the Sun is low in the cooker is not useful.
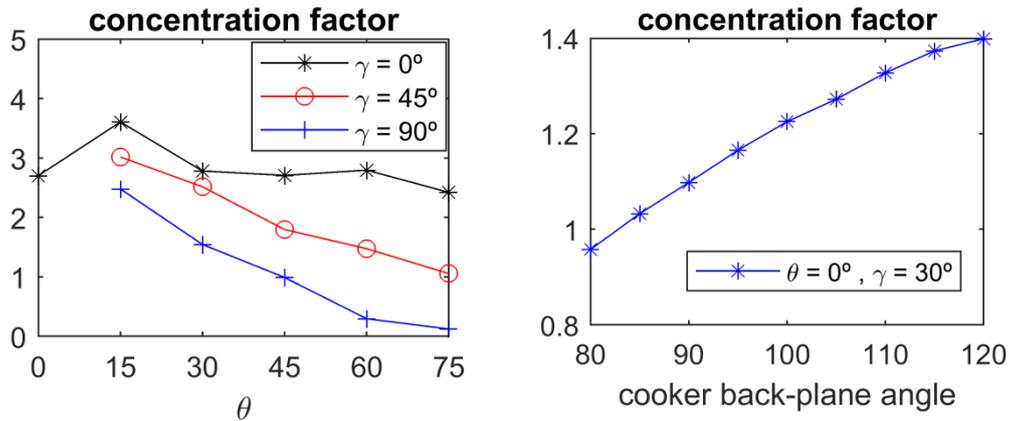
Figure 4. Left: Concentration factor for the total irradiation in the cooking vessel as a function of the position of the Sun in the sky (given by angles θ and γ). Right: Concentration factor as a function of the inclination of the back panel of the solar cooker.

Figure 4 (right) illustrates the effect in the concentration ratio of the inclination of the back panel of the funnel cooker; in our input file the shape of the cooker is always continuous at the edges of the polygons, so this angle controls the amount of parabolicity. For a fixed position of the Sun of $\theta = 0°$ (summer) and $\gamma = 30°$ (before midday, cooking for the lunch), cf. Fig. 3 (right), the concentration factor is larger as more open are the panels of the cooker.

10. CONCLUSIONS

This paper has presented a prototype software for the simulation of solar panel cookers by means of the radiosity method. The geometry of the solar cooker, cooking vessel and transparent cooking enclosure is approximated by plane polygons in three dimensions, by using an input text file. The Sun position in the sky relative to the cooker can also be selected, so the transitory evolution of the heat transfer during the cooker operation can be estimated. The sky can also emit a part of the total radiation. For validation, a simplified solar panel cooker has been simulated under several situations. The results presented in this work are preliminary, but apparently are consistent with the expectations.

Future work is in progress, with emphasis in the validation of the software by means of real experiments with panel solar cookers. Additionally, the prototype software will be improved with a graphical interface for the generation of the input files. Finally, a future comparison with the ray-tracing method will be accomplished.

ACKNOWLEDGEMENTS

REFERENCES

[1] Muthusivagami RM, Velraj R, Sethumadhavan R. Solar cookers with and without thermal storage—A review. Renewable and Sustainable Energy Reviews, 2010, 14: 691-701.

[2] Cuce E, Cuce PM. A comprehensive review on solar cookers. Applied Energy, 2013, 102:1399-1421.

[3] Ruivo CR. Solar cooking is feasible, it is not a myth. International Journal of Engineering and Management Research (IJEMR), 2018, 8: 1-6.

[4] Chejne F, Macía A, Estrada D, Velásquez HI, Londoño C. Radiation model for predicting temperature evolution in solar cooker. Dyna, 2011, 166: 68-74.

[5] Siegel R, Howell JR. Thermal radiation heat transfer, Taylor & Francis, 4th ed., 2002.

[6] Cohen MF, Wallace JR. Radiosity and realistic image synthesis, Academic Press, 1993.

[7] Bradley W. Reciprocal optical test for measuring solar cooker performance.
    http://www.solarcookers.org/files/5414/2747/1563/Reciprocal_Optical_Test.pdf

[8] Yettou F, Azoui B, Malek A, Gama A. Study and simulation of concentrating irradiance in box solar cooker with tracking reflectors. Revue des Energies Renouvelables, 2012, 15: 661-670.

[9] McCluney R. Solar cooker reflector optical evaluation and design evolution. FSEC Solar Cooker Report, 2001. http://www.fsec.ucf.edu/en/publications/pdf/FSEC-GP-214-01.pdf

[10] Tan T. Fun-Panel. The Solar Cooking Wiki, 2013.
     http://solarcooking.wikia.com/wiki/Fun-Panel

[11] Ruivo CR. Celestino Solar Funnel Cooker. The Solar Cooking Wiki, 2012.
     http://solarcooking.wikia.com/wiki/Celestino_Solar_Funnel_Cooker